Catalyst interfacial step flow drives the nucleation of carbon nanotubes

Rahul Rao[1], Renu Sharma[2], Frank Abild-Pedersen[3], Jens K. Norskov[3,4], Avetik R. Harutyunyan[1]*

[1]*Honda Research Institute USA Inc., Columbus, Ohio, 43212, USA*

[2]*Center for Nanoscale Science and Technology, National Institute of Standards and Technology, Gaithesburg, Maryland, 20899, USA*

[3] *SUNCAT Center for Interface Science and Catalysis, SLAC National Accelerator Laboratory, Menlo Park, CA, USA*

[4]*Department of Chemical Engineering, Stanford University, Stanford, CA, 94305, USA*

Abstract

Fulfilling the strong demand of carbon nanotubes (CNT's) with desirable characteristics requires understanding of their growth mechanism in the early cap nucleation stage when the symmetry is set. Here we present real-time atomic-scale observation of nanotube cap nucleation on nickel nanocatalyst by using transmission electron microscopy. The nucleation begins by the creation of a graphene embryo bounded between opposite step edges on the catalyst surface. The embryo evolves into a cap when at least one of the steps flows and crosses the edges of adjacent facets on the catalyst tip. Further motion of the steps away from the catalyst tip with attached rims of carbon cap generates the tubular wall of the nanotube. Through Density Functional Theory calculations we attribute this surface restructuring to the surface self-diffusion of catalyst atoms via a step-edge attachment-detachment mechanism. Our results suggest an interrelationship between the structures of adjacent facets as the dominant factor in cap nucleation, and thereby symmetry formation of the nanotube.

Controlled growth of carbon nanotubes with desired properties is imperative for their unique applications[1,2], which in turn requires a full understanding of their growth mechanism. In particular, an understanding of the cap nucleation stage still remains a challenging task. Towards this end, earlier work by Helveg et al.[3] was a substantial contribution to the field where the early stage of catalytic formation of graphitic carbon layers was captured *in situ* by environmental transmission electron microscopy (ETEM) and provided important hints into the growth mechanism of carbon nanofibers. *In situ* ETEM studies have revealed reaction-induced reshaping of Ni catalyst particles by the restructuring of monoatomic step edges. This observation, combined with theoretical modeling, suggested that step-edge sites act as the preferential growth centers for graphitic layers on the Ni surface [3-5]. The *in situ* results also agreed with earlier theoretical predictions .[5]

However, these observations on carbon nanofiber growth do not easily extend to carbon nanotubes[6]. The nucleation of a carbon nanotube within an ETEM was observed later by the injection of carbon atoms from graphitic shells surrounding the metal catalyst particle into the body of the particle by electron beam irradiation.[7] This event was also accompanied by dynamic morphological changes of catalyst particle (Fe) during tube growth, suggesting wetting-driven deformation of the particle tip into a convex dome as a necessity for the formation of the carbon nanotube cap[7]. In parallel, other ETEM studies have revealed more insights into the CNT growth mechanism and also demonstrated examples of catalyst reconstruction and surface steps bounding by nanotube rims[8-13]. The majority of the researchers that have targeted this problem attest to the key roles of catalyst size and symmetry in the formation of nanotube symmetry based on observations such as the

correlation between the nanotube wall basal plane and the structure of the corresponding facet on the catalyst, the impact of catalyst composition and pretreatment conditions on the structure of the nanotubes, and the selectivity of the growth kinetics for nanotube with various chiral indexes.[13-20]

In spite of the large number of *in situ studies* capturing the early stages of CNT growth, specifically, the atomic scale nucleation of the carbon nanotube cap has never been observed and its mechanism still remains unclear. The nanotube cap, by virtue of its geometry necessitates the creation of pentagons in the hexagonal sp^2 lattice, which enables it to conform to the curvature of the catalyst particle tip.[21]. Thus the structure of the cap is inherently different from a bent graphene layer, which has been observed previously. The cap formation stage is central for establishing the nanotube structure chiral indexes[21], and the understanding of the cap formation mechanism is critical towards controllable growth of carbon nanotubes. Two of the experimental challenges that have thus far precluded the direct observation of cap formation are the difficulty in locating a particular catalyst that is capable of CNT nucleation, and the very short nucleation times, especially in the case of single-walled nanotubes (SWNTs). In the present work we overcame these obstacles by atomic-scale imaging of cap nucleation of the innermost tube during catalytic growth of multi-walled nanotube (MWNT) at low temperature. Precise knowledge of the catalyst particle tip location made it possible to detect and follow the kinetics of the initial stage of growth of the innermost tube in the MWNT. The space between the surface of the catalyst particle and the previously grown nanotube was thus used as a nanoscale reactor inside which we observed the nucleation of the new inner tube as a SWNT. We found that catalyst surface step flow through the adjacent facets first introduces

curvature on a graphene embryo that is constrained between opposite steps. The embryo subsequently emerges as carbon cap in the course of step flow away from the catalyst tip. Our observation emphasizes the essential role of graphene embryo-catalyst step interface in the formation of nanotube symmetry.

Results

Observation of carbon nanotube cap nucleation

The MWNTs were grown on Au-doped Ni nanoparticles (10 to 15 nm) at 520 ^{o}C using acetylene (C_2H_2) as the carbon source (see Methods and Ref. [22] for more details). Under these conditions, CNT growth occurred by the tip-growth mode, eliminating the possibility of catalyst shape reconstruction induced by interaction with a substrate. Furthermore, the low growth temperature (520 °C) provided a relatively slow growth rate (≈1 nm/s) and allowed the catalyst particle to preserve its crystallinity during CNT growth. Hence, the catalyst shape changes observed during the experiment were induced only by the decomposition of the carbon feedstock and adsorption of carbon on the catalyst surface. Figs. 1a and 1b show high-resolution snapshots captured just after cap lift-off and during elongation of the innermost tube (indicated by white arrows) within the MWNT. The particle shape changes accompanying tube growth can be clearly seen. Fast Fourier transform (FFT or diffractogram) analysis of the crystalline particle revealed its structure to be Ni_3C (Fig. 1c). The facets on the particle are assigned as $(\bar{1}\bar{1}2)$, $(\bar{1}0\bar{3})$, and $(1\bar{1}0)$ (Fig. 1d).

Time-resolved high-resolution images from a digital video sequence capturing the nucleation of the inner tube within a MWNT (Supplementary Information, Video 1) are shown in Fig. 2. A high video frame rate (15 s^{-1}), coupled with the low CNT growth rate provided the temporal resolution to observe the nucleation of the innermost tube and associated catalyst morphology changes. We chose the time t = 0 as just before the graphene embryo formation was observed on the surface of the catalyst particle. As shown by the sequence of images and the corresponding schematics in Fig. 2, the cap formation of the new inner nanotube begins with the formation of a graphene embryo on the $(\bar{1}\bar{1}21)$ facet of the catalyst particle (Fig. 1a). The embryo is bound on both sides by steps on the surface of the catalyst particle (indicated by the white arrow in Fig. 2). The two steps have opposite signs and start to flow in opposite directions on the particle surface, causing elongation of the graphene embryo. Such motion of graphene layers bounded by catalyst steps is also reported in Ref. 9. Remarkably, by t = 0.3 s (Fig. 2b), the step on the right reaches the end of the facet and crosses over to the adjacent facet which is at an angle of ≈ 60° to the $(\bar{1}\bar{1}21)$ facet. The graphene embryo can be seen clearly attached to the step (indicated by the black arrows in Fig. 2). The interfacial motion of the step across the particle tip surface introduces curvature into the growing graphene embryo. This curvature increases as the step crosses over another adjacent facet (Fig. 2f) leading to nanotube cap formation. Over the next few seconds both steps keep moving simultaneously away from particle tip, leaving behind the nanotube cap bound to the particle. Detachment (lift-off) of the cap occurs after several seconds due to reconstruction of the particle facets under the cap. The nascent nanotube can be seen in Fig. 2g.

Step flow

The observation of nanotube cap nucleation described above highlights the importance of not only the structure of catalyst, but also the inter-relationships between the adjacent facets during the initial stage of growth. It is established that carbon adsorption and degree of coverage lead to the surface reconstruction of the catalyst particle, which varies depending on the structure of the facets.[12,23] Since the arrangement of steps on the surface defines particle morphology, step flow is one of the most likely mechanisms through which the surface reconstruction takes place. The presence of steps on a crystal surface are common and can occur by thermal fluctuations of edge atoms, leading to their detachment[24]. Such steps and kinks are also likely to be present on the surfaces of smaller particles[25]. Surface steps can also be induced by adatoms (e.g. carbon) adsorption[24], since the carbon binding energy to the Ni step is larger than the energy cost for step formation[5] and are known to be high reactivity sites.[26] Hence in our experiment, carbon adsorption, either on steps or on terraces, followed by graphene embryo formation causes a variation in the surface energies of facets. Consequently, in order to equilibrate the catalyst surface undergoes reconstruction through the step flow, which in turn causes further development of the attached graphene embryo into a nanotube (Fig. 2).

One of the distinguishing features of CNT nucleation from the formation of graphene layers during growth of carbon fibers described in Ref. 3 is that in order to produce a nanotube the simple extension or bending of the graphene embryo around the catalyst particle is not enough – It first needs to form a cap on the catalyst tip. As shown in Fig. 2 the cap formation is

realized only when the step flows over adjacent facets on the catalyst tip followed by lift-off due to the surface reconstruction. This unique mechanism of cap formation puts certain restrictions on the symmetries of adjacent facets and thus on the corresponding steps and terraces. This necessitates appropriate relationships between the structures of adjacent facets in order to maintain the high degree of symmetry of the growing nanotube. The exact mechanism is yet to be understood in detail. Indeed, Density Functional Theory (DFT) calculations of graphene growth on metal surfaces have shown that the preferential nucleation sites for carbon embryo (step edges or terrace) not only depends on the nanocatalyst composition and symmetry (for example FCC, BCC or HCP), but also the corresponding facet symmetry within the catalyst.[27] Moreover, the lowest critical size of a graphene embryo also depends on the facet (step/terrace) symmetry, which was concluded based on competition between the energy cost of graphene embryo edges and formation of thermodynamically stable bulk graphene layer[5,27]. Hence, from a thermodynamic viewpoint, cap formation can occur on a surface of the particle tip via step flow if the symmetries of adjacent facets and their step edges satisfy the conditions where carbon atoms bind most favorably to the step edges. In addition, the initial step-bound graphene embryo must be stable so that it can grow. Finally, the interrelated sequence of facet symmetries should be favorable for cap lift-off upon reconstruction[12].

Next, we would like to point out interesting events that were observed during the growth of the MWNT in the ETEM. In addition to step-mediated initial nucleation of a nanotube cap, we observe three different morphologies formed on the catalyst surface as a result of step flow processes resulting in termination of nanotube growth. Fig. 3a demonstrates the first

scenario where the step flow (with the attached nanotube wall) towards the carbon-free end of the particle caused the eventual flattening of the step. This in turn leads to the detachment of the nanotube wall (black arrow), and consequently, termination of growth. This type of growth termination is particularly more prevalent in bamboo-shaped or herringbone-shaped nanotubes and was observed also in case of carbon fiber growth[3]. The second scenario we observe is that nanotube rim remains attached even after flattening of corresponding step, causing the attached wall to become bent (Fig.3b), which has also been observed previously in MWNTs[7,28]. The many walls of a MWNT are also most commonly observed attached to several densified steps at the end of growth (Fig.3c, d). In this case the terrace lengths are significantly shorter in comparison to their lengths at the beginning stages of CNT growth. We attribute this observation to the phenomenon known as step bunching, which occurs when the steps on the vicinal facets of a crystal surface become perturbed due to kinetic instabilities that destabilize a uniform step train, [29-31] causing the steps to bend or aggregate together. In our case one could consider destabilization of the step train as a result of adsorbed carbon adatoms and thereby model the step bunching phenomena during CNT growth by applying impurity-induced step bunching mechanisms proposed first by Frank[29] and further developed by others later[32-34]. However, these models assume non-interacting impurities in front of a step that impedes its motion. In the case of CNT growth, the carbon adatoms (impurities) bond with each other and form a graphene layer that is attached to the steps and covers the entire upper and lower terraces depending on the instant of growth. Thus the models described above cannot be applied. Theoretical modeling of our observations would surely provide greater understanding of the cap nucleation mechanism, yet this would be a daunting task for the present work

considering the complications and the fact that it took decades for the development of existing various models.

Discussion

Although a complete theoretical modeling of graphene-bound step flow kinetics is not possible, it is still possible to discuss the path of the mass flow mechanism during Ni surface reconstruction, which can be important to understand rate limiting processes during nanotube growth. As shown in Figs. 2 and 3, a graphene layer (cap or wall) is bound to steps and covers the terrace. Since the binding energy between Ni and carbon based on experimental results (≈7 eV)[35] appears stronger than the Ni-Ni bond (≈2.3 eV)[36], step motion could occur by surface self-diffusion or attachment-detachment of Ni atoms from the step only during the growth of a MWNT. There are two ways in which the step-based growth of MWNT can proceed and both involve the diffusion of Ni atoms away from the step-edge. Fig. 4 shows the schematics of the different possible processes: (1) bulk diffusion (Fig. 4a), and (2), diffusion of a Ni atom under the graphene sheet (blue arrow in Fig. 4b) or up on the terrace under another sheet (red arrow in Fig. 4b). We have performed DFT calculations of Ni atom diffusion on Ni (111) surfaces (**note Ni but not NiC**) to identify which of the two possible routes are most feasible. We note that while the particle studied here is in the carbide form, we considered pure metal catalyst for the calculation since the necessary interatomic potentials and other details are more readily available. For the metal particle mediated process we have found that diffusion of a Ni atom between two bulk or subsurface interstitial sites is associated with a barrier of less than 0.2 eV

in both processes. However, the energy differences between having a Ni atom on the Ni(111) surface or in the subsurface or bulk interstitial sites are 2.4 eV and 4.8 eV, respectively. This indicates that surface diffusion of Ni atoms is more likely to play a significant role in the catalyzed growth of carbon nanotubes. In a prior DFT study it was shown that the graphene sheet enhanced the stability of atomic Ni on the surface and that the attachment-detachment of Ni from the step-edge during carbon incorporation in the growing fiber had a barrier of less than 0.6 eV.[4] Hence, the surface mediated process is associated with much lower energy barriers and the mechanisms shown in Fig. 4b are enough to facilitate continued growth of the carbon nanotubes.

In summary, we describe the CNT nucleation process by the following sequence: 1) Formation of steps on the catalyst surface via carbon adsorption (or precipitation of carbon at pre-existing steps); 2) Growth of a graphene embryo constrained by neighboring steps with opposite signs; 3) Formation of the nanotube cap by step flow over adjacent facets of the catalyst tip; 4) Elongation of the cap via further steps flow away from the catalyst tip. We draw the following conclusions from this model: 1) The structural inter-relationship between adjacent facets on catalyst tip should be feasible for cap nucleation; 2) Step flow during MWNT growth occurs via surface self-diffusion of catalyst atoms and is a rate limiting process for nucleation; 3) In general MWNT growth is accompanied by step bunching phenomenon on catalyst surface. A word of caution is needed however: depending on catalyst composition and symmetry of particular facets there could also be a scenario where carbon binding with the terrace is more preferable than with the step edge[27]. In this case any epitaxial relationship between the nanotube and catalyst would be between the graphene basal plane and catalyst

terrace. Our study implies a self-consistent relationship between catalyst reconstruction and cap nucleation in the manner that the catalyst surface morphology and interrelationship between facet symmetries defines the feasibility of cap formation, while the nucleated cap is responsible for the structural symmetry of the nanotube.

Methods

Thin films of Ni (≈1 to 2 nm thick, with a small amount of Au[18]) were first deposited on perforated SiO_2 films supported on 200 mesh Mo TEM grids by physical vapor deposition. The grids were loaded on a TEM heating holder and introduced to the ETEM column. Upon heating (> 200 °C) the films dewetted from the SiO_2 substrate to form 4 to 7 nm diameter particles. The size of the particles did not change appreciably upon further heating to the reaction temperatures used (520 °C). Samples were held at the reaction temperature for ≈ 25 min. in order to stabilize the temperature and fully reduce any NiO (if present) to Ni. C_2H_2 was then introduced into the ETEM to induce CNT growth. A pressure of ≈ 0.4 Pa was maintained during the growth period of 15 min.

After every in situ growth experiment, we record images from regions not exposed to the electron beam during the experiment at room temperature and in high vacuum. We compare the images of the tubes/catalyst particle with the ones recorded during growth and find no difference. Therefore, based on this level general capability and fact that our irradiation was carried out at beam current densities ≈10A$(cm^2)^{-1}$, while even in case of 10^3-10^5A$(cm^2)^{-1}$ current densities atomic displacement was observed only from MWNTs but not from metal

particles due to the high displacement threshold energy in metals[37-39] we exclude electron irradiation effects during the nanotube growth process under our experimental conditions.

References

1 Avouris, P., Chen, Z. & Perebeinos, V. Carbon-based electronics. *Nature Nanotech.* **2**, 605-615 (2007).

2 De Volder, M. F. L., Tawfick, S. H., Baughman, R. H. & Hart, A. J. Carbon Nanotubes: Present and Future Commercial Applications. *Science* **339**, 535-539 (2013).

3 Helveg, S. *et al.* Atomic-scale imaging of carbon nanofibre growth. *Nature* **427**, 426-429 (2004).

4 Abild-Pedersen, F., N√∏rskov, J. K., Rostrup-Nielsen, J. R., Sehested, J. & Helveg, S. Mechanisms for catalytic carbon nanofiber growth studied by ab initio density functional theory calculations. *Phys. Rev. B* **73**, 115419 (2006).

5 Bengaard, H. S. *et al.* Steam Reforming and Graphite Formation on Ni Catalysts. *J. Catal.* **209**, 365-384, doi:http://dx.doi.org/10.1006/jcat.2002.3579 (2002).

6 Ajayan, P. M. Nanotechnology: How does a nanofibre grow? *Nature* **427**, 402-403 (2004).

7 Rodriguez-Manzo, J. A. *et al.* In situ nucleation of carbon nanotubes by the injection of carbon atoms into metal particles. *Nature Nanotech.* **2**, 307-311 (2007).

8 Lin, M. *et al.* Dynamical Observation of Bamboo-like Carbon Nanotube Growth. *Nano Lett.* **7**, 2234-2238, doi:10.1021/nl070681x (2007).

9 Hofmann, S. *et al.* In situ Observations of Catalyst Dynamics during Surface-Bound Carbon Nanotube Nucleation. *Nano Letters* **7**, 602-608, doi:10.1021/nl0624824 (2007).

10 Yoshida, H., Takeda, S., Uchiyama, T., Kohno, H. & Homma, Y. Atomic-Scale In-situ Observation of Carbon Nanotube Growth from Solid State Iron Carbide Nanoparticles. *Nano Letters* **8**, 2082-2086, doi:10.1021/nl080452q (2008).

11 Begtrup, G. E. *et al.* Facets of nanotube synthesis: High-resolution transmission electron microscopy study and density functional theory calculations. *Phys. Rev. B* **79**, 205409 (2009).

12 Pigos, E. *et al.* Carbon Nanotube Nucleation Driven by Catalyst Morphology Dynamics. *ACS Nano* **5**, 10096-10101, doi:10.1021/nn2040457 (2011).

13 Fiawoo, M. F. C. *et al.* Evidence of Correlation between Catalyst Particles and the Single-Wall Carbon Nanotube Diameter: A First Step towards Chirality Control. *Phys. Rev. Lett.* **108**, 195503 (2012).

14 Chiang, W.-H. & Sankaran, R. M. Linking Catalyst Composition to Chirality Distributions of As-grown Single-walled Carbon Nanotubes by Tuning NixFe1-x Nanoparticles. *Nature Mater.* **8**, 1-5, doi:10.1038/nmat2531 (2009).

15 Harutyunyan, A. R. *et al.* Preferential Growth of Single-Walled Carbon Nanotubes with Metallic Conductivity. *Science* **326**, 116-120 (2009).

16 Liu, J. *et al.* Chirality-controlled synthesis of single-wall carbon nanotubes using vapour-phase epitaxy. *Nat. Commun.* **3**, 1199 (2012).

17 Ding, F., Harutyunyan, A. & Yakobson, B. Dislocation theory of chirality-controlled nanotube growth. *Proc. Nat. Acad. Sci.* **106**, 2506 (2009).

18 Zhu, H. *et al.* Atomic-Resolution Imaging of the Nucleation Points of Single-Walled Carbon Nanotubes. *Small* **1**, 1180-1183, doi:10.1002/smll.200500200 (2005).

19 Koziol, K. K. K., Ducati, C. & Windle, A. H. Carbon Nanotubes with Catalyst Controlled Chiral Angle. *Chem. Mater.* **22**, 4904-4911, doi:10.1021/cm100916m (2010).

20 Harutyunyan, A. R. The catalyst for growing single-walled carbon nanotubes by catalytic chemical vapor deposition method. *J. Nanosci. Nanotech.* **9**, 2480-2495 (2009).

21 Reich, S., Li, L. & Robertson, J. Structure and formation energy of carbon nanotube caps. *Phys. Rev. B* **72**, 165423 (2005).

22 Sharma, R., Chee, S.-W., Herzing, A., Miranda, R. & Rez, P. Evaluation of the Role of Au in Improving Catalytic Activity of Ni Nanoparticles for the Formation of One-Dimensional Carbon Nanostructures. *Nano Lett.* **11**, 2464-2471, doi:10.1021/nl2009026 (2011).

23 Moors, M. *et al.* Early Stages in the Nucleation Process of Carbon Nanotubes. *ACS Nano* **3**, 511-516, doi:10.1021/nn800769w (2009).

24 Somorjai, G. A. & Van Hove, M. A. Adsorbate-induced restructuring of surfaces. *Progress in Surface Science* **30**, 201-231, doi:http://dx.doi.org/10.1016/0079-6816(89)90009-9 (1989).

25 Lang, B., Joyner, R. W. & Somorjai, G. A. Low energy electron diffraction studies of chemisorbed gases on stepped surfaces of platinum. *Surface Science* **30**, 454-474, doi:http://dx.doi.org/10.1016/0039-6028(72)90012-X (1972).

26 Vang, R. T. *et al.* Controlling the catalytic bond-breaking selectivity of Ni surfaces by step blocking. *Nature Mater.* **4**, 160-162 (2005).

27 Saadi, S. *et al.* On the Role of Metal Step-Edges in Graphene Growth. *J. Phys. Chem. C* **114**, 11221-11227, doi:10.1021/jp1033596 (2010).

28 Pohl, D. *et al.* Understanding the Metal-Carbon Interface in FePt Catalyzed Carbon Nanotubes. *Phys. Rev. Lett.* **107**, 185501 (2011).

29 Frank, F. C. in *Proceedings of the International Conference Crystal Growth* (eds R. Doremus, B. Roberts, & D. Turnbull) (Wiley, 1958).

30 Schwoebel, R. E. & Shipsey, E. J. Step Motion on Crystal Surfaces. *J. Appl. Phys.* **37**, 3682-3686 (1966).

31 Schwoebel, R. E. Step Motion on Crystal Surfaces II. *J. Appl. Phys.* **40**, 614-618 (1969).

32 Eerden, J. P. v. d. & Muller-Krumbhaar, H. Dynamic Coarsening of Crystal Surfaces by Formation of Macrosteps. *Phys. Rev. Lett.* **57**, 2431-2433 (1986).

33 Kandel, D. & Weeks, J. D. Step motion, patterns, and kinetic instabilities on crystal surfaces. *Phys. Rev. Lett.* **72**, 1678 (1994).

34 Kandel, D. & Weeks, J. D. Theory of impurity-induced step bunching. *Phys. Rev. B* **49**, 5554 (1994).

35 Isett, L. C. & Blakely, J. M. Binding of carbon atoms at a stepped - Ni surface. *Journal of Vacuum Science and Technology* **12**, 237-241 (1975).

36 Kant, A. Dissociation Energies of Diatomic Molecules of the Transition Elements. I. Nickel. *Journal of Chemical Physics* **41**, 1872 (1964).

37 Banhart, F. Irradiation effects in carbon nanostructures. *Reports in Progress in Physics* **62**, 1181 (1999).

38 Sun, L. *et al.* Carbon Nanotubes as High-Pressure Cylinders and Nanoextruders. *Science* **312**, 1199-1202 (2006).

39 Rodriguez-Manzo, J. A. *et al.* Heterojunctions between metals and carbon nanotubes as ultimate nanocontacts. *Proc. Nat. Acad. Sci.* **106**, 4591-4595 (2009).

Acknowledgements

We thank A. Zangwill for helpful discussions and advice on this manuscript, (continue)…

This research was supported by the Honda Research institute USA Inc.

Author contributions

R.R. analyzed the data, R.S. performed the TEM experiments and helped with data analysis, F. A-P. and J.K.N. performed DFT calculations, A.R.H. initiated and designed the research and analyzed the data. R.R. and A.R.H. wrote the paper.

Figure Legends

Figure 1. *In situ* TEM images recorded during MWNT growth. (**a**,**b**) High-resolution TEM images recorded just after lift-off of the innermost tube inside a MWNT (**a**), and during elongation of the tube (**b**). The innermost tube is indicated by a white arrow in (**a**) and (**b**). (**c**) High magnification view of the catalyst particle tip just after lift-off of the innermost tube inside the MWNT. The FFT (inset in **c**) from the particle can be indexed to the $(1\bar{1}0)$ spacing from Ni_3C. (**d**) The same view as in (**c**) with the facet structures indicated. The structures of the neighboring facets were estimated from the angles between the planes according to the Ni_3C crystal structure. All scale bars in the figure are 2 nm.

Figure 2. Image sequence captured from Video 1 showing nanotube cap formation. Images (**a**-**g**) show the process of nanotube cap formation followed by lift-off. Schematics are included with each figure to show the elongation of the graphene embryo bound to steps on the $(\bar{1}\bar{1}21)$ facet of the catalyst particle. The white and black arrows indicate the step and nanotube cap, respectively. The scale bar is 5 nm.

Figure 3. Step flow-induced termination of CNT growth and step bunching. (**a**) TEM image showing detachment of the outer wall (indicated by the black arrow) and termination of growth

due to flattening of the step. (**b**) TEM image showing bending of the nanotube wall at the attachment point to the step. The scale bar is 5 nm. (**c**) High-resolution image captured the agglomeration of the steps with attached MWNT walls (**d**) The same view as in (**c**) with a dotted line outlining the step structure as a guide to the eye. The structure of the step closest to the particle surface (indicated by the white arrow) can be indexed as $(1\bar{1}3)$. Scale bar in the figure is 2 nm.

Figure 4. Nickel atom diffusion during CNT growth. Schematics showing the pathways for, (**a**) subsurface (or bulk) diffusion and, (**b**) surface diffusion of Ni atoms during step flow when the step is connected to a MWNT. The latter involves two possible scenarios in which both are identical in their final state energy. The Ni step-edge atom can be pushed onto the upper terrace (red arrow) or under the growing graphene layer (blue arrow). CNT growth is expected to proceed via the process involving Ni detachment under the graphene layer due to the enhanced stability induced by the graphene layer.

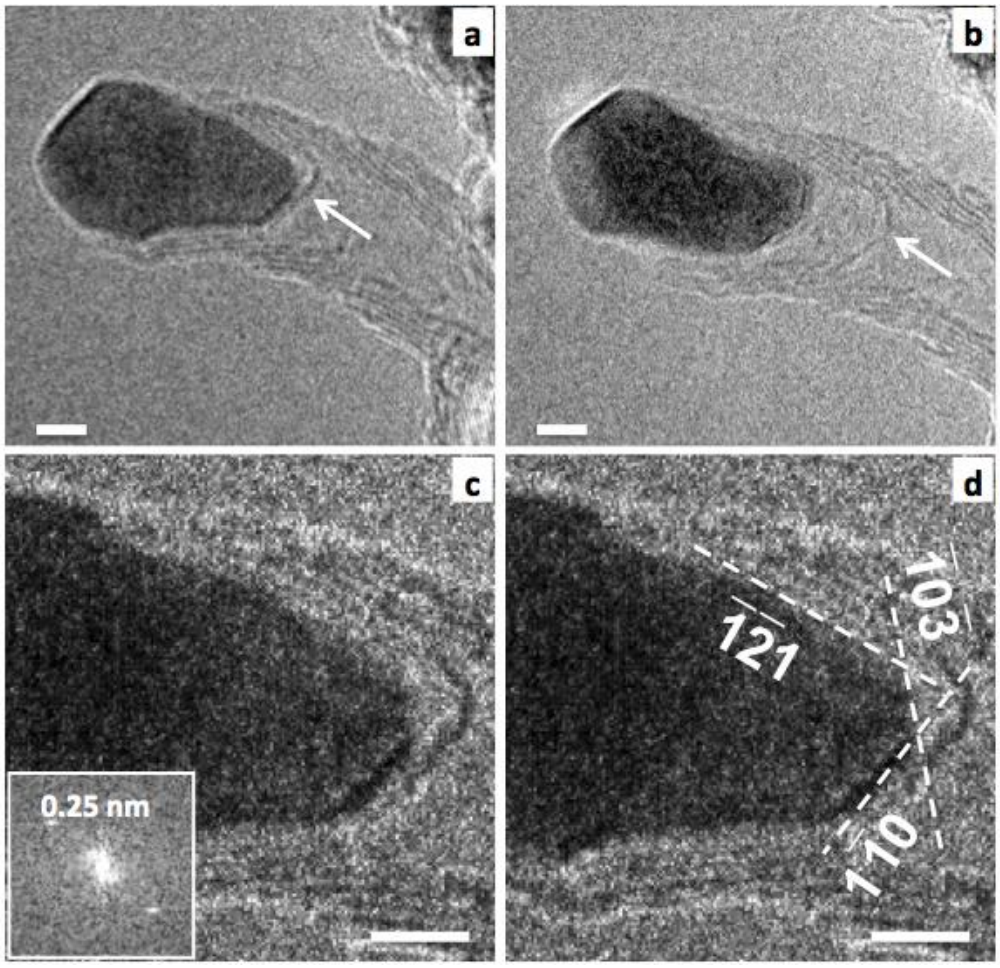

Figure 1.

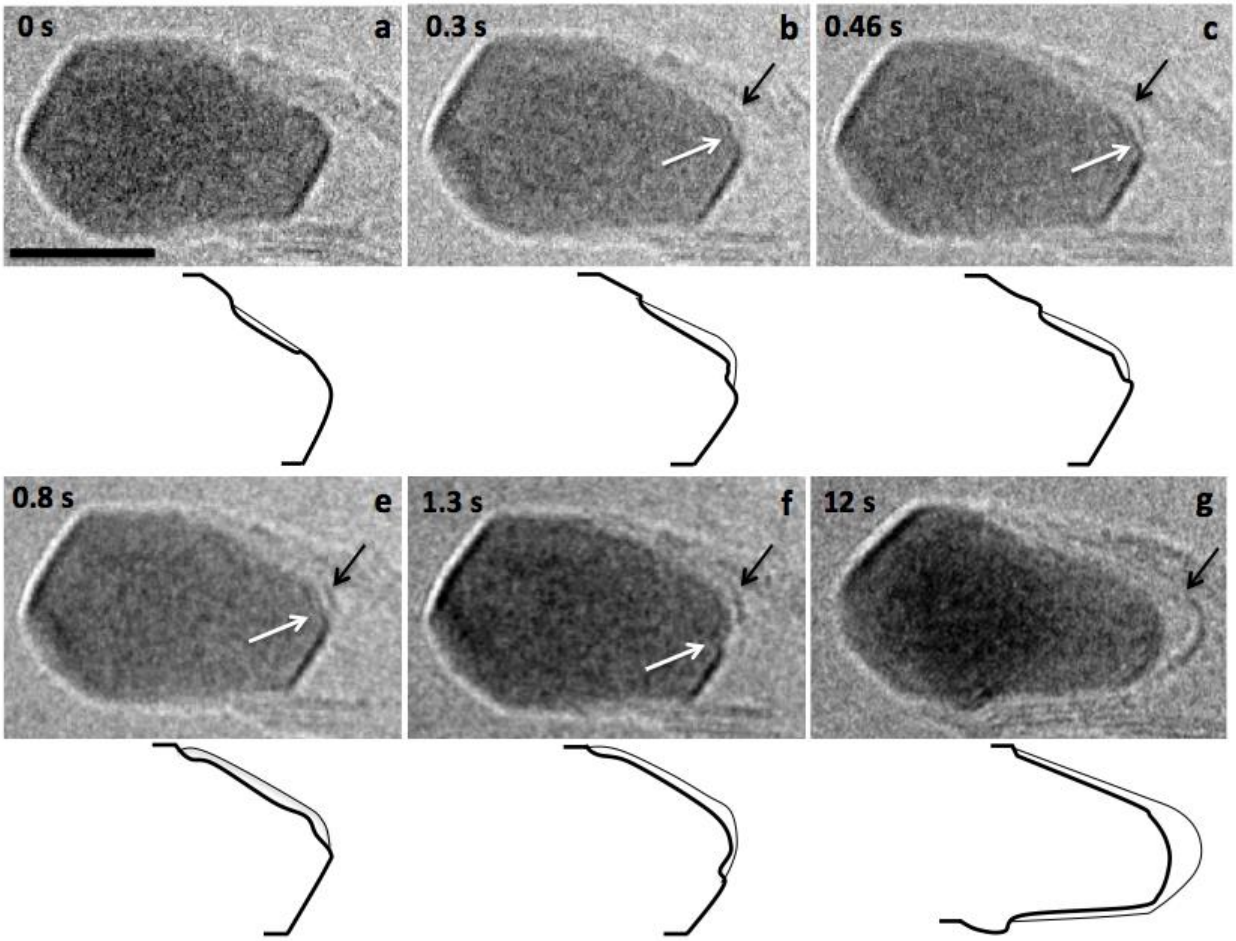

Figure 2.

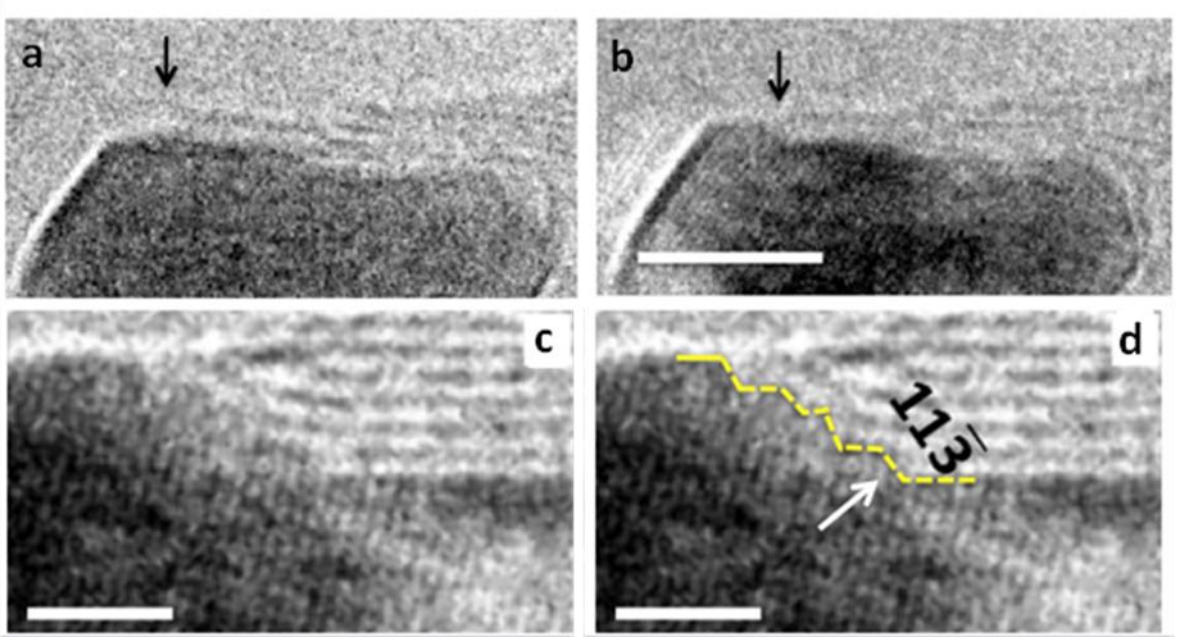

Figure 3

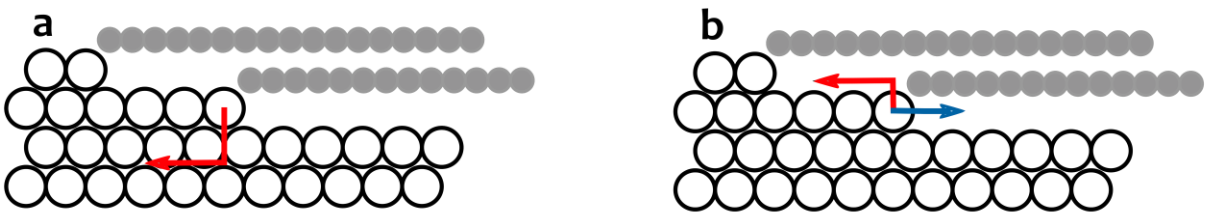

Figure 4.